

Thermal differences between right and left portions of air-convection crushed-rock embankment in permafrost regions



Yanhu Mu, Wei Ma, Guoyu Li & Yongzhi Liu

State Key Laboratory of Frozen Soils Engineering, Cold and Arid Regions Environmental and Engineering Research Institute, Chinese Academy of Sciences, Lanzhou, Gansu, China

Yuncheng Mao

Gansu Provincial Communications Research Institute Co., Ltd.

ABSTRACT

The right and left slopes of air-convection crushed-rock embankment (ACCE) commonly experience considerable thermal differences in permafrost regions. Those thermal differences could lead to an asymmetrical thermal regime within and beneath the ACCE, and then result in different deformations on the embankment. Based on in situ ground temperature along the Qinghai-Tibet Railway, this paper chose three monitoring sites of U-shaped air-convection crushed-rock embankment with different orientations to analysis the thermal differences between right and left portions of the embankment and underlying permafrost. The analysis included comparisons of temperatures, n-factors, freezing and thawing indices of near-surface grounds on the embankment shoulders and the natural grounds, and also includes the relationships between the thermal differences and solar radiation and wind-forced convection of the embankment. Finally, two different conditions of the thermal regime beneath the embankment were presented by ground temperature profiles of the embankment shoulders and the natural grounds. The results indicated that for the embankment with orientation of near north to south, the thermal differences was small and thus thermal regime beneath the embankment was almost symmetrical; but for embankment with orientation of near east to west, induced by single or double effects of the solar radiation and the wind-forced convection, the thermal differences were significant and consequently led to a severe asymmetrical thermal regime beneath the embankment.

RÉSUMÉ

Un gradient thermique considérable existe entre les pistes gauche et droite de l'air de convection écrasés-rock remblai(ACCE) dans les régions du pergélisol.Ce gradient, accumulant sur le hauteur de l' ACCE, aboutit dans un premier temps à un régime thermique asymétrique à l'intérieur et au-dessous de l'ACCE. Ce phénomène génère aussi des déformations différentes dans les régions du pergélisol, et finalement influence la stabilité du remblai. A partir des données de la température du sol sur le chemin de fer de Qinghai-Tibet, cet article choisit trois sites de surveillance de l'air de convection écrasés-rock remblai en forme de U(USACCE), avec de différentes orientations du remblai et de différente température moyenne annuelle du sol, pour analyser les différences thermiques entre les pistes gauche et droite du remblai et le pergélisol sous-jacent. L'analyse comprend des comparaisons des températures, n-facteurs, le gel et le dégel des indices au sol près de la surface à la gauche et droite des épaules remblai et la surface naturelle du sol, et également les relations entre les gradientss thermiques, le rayonnement solaire et vent-convection de l'USACCE. Finalement, deux conditions différentes du régime thermique au-dessous du remblai sont présentés par des comparaisons entre les profils de la température du sol à la gauche et droite des épaules remblai et le sol naturel. Les résultats des analyses et comparaisons montrent que les gradients thermiques entre le sol près de la surface à la gauche et droite des épaules remblai sont insuffisantes pour les remblais à la orientation près du nord au sud, et donc le régime thermique au-dessous du remblai est presque symétrique. Mais pour les remblais à la orientation près du est au ouest, les gradients thermiques entre le sol près de la surface à la gauche et droite des épaules remblai sont importants et le régime thermique au-dessous du remblai est asymétrique, à cause des influences des effets uniques ou doubles du rayonnement solaire et du vent-convection de l'USACCE.

1 INTRODUCTION

As a method of providing cooling, air-convection crushed-rock embankment (ACCE) had been employed widely along the Qinghai-Tibet Railway (QTR) in permafrost regions, and performed well in protecting the underlying permafrost from warming and thawing (Cheng et al., 2008; Ma et al., 2006; Wu et al., 2008). Crushed-rock layer of the ACCE, acting as a thermal semi-conductor (Cheng et al., 2007), can actively lower ground temperatures within the embankment and underlying permafrost. In winter, Raleigh–Bernard convection takes place in the crushed-rock layer where ambient air being

colder than soil in the embankment, results in a substantial heat loss of soil in and beneath the embankment; in summer, the heat exchange between the atmosphere and the embankment is dominated by thermal conduction as the ambient air is warmer than soil in the embankment. But this conduction is less effective and thus the heat into the embankment is small due to the low thermal conductivity of the void air and small contact areas among the crushed-rock layer. Via the winter convection and the summer conduction, the ACCE produces a net heat loss of soil in and beneath the embankment on an annual basis and therefore cools underlying permafrost (Cheng and Tong, 1978; Cheng et

al., 2008; Goering, 2003; Goering and Kumar, 1996). U-shaped air-convection crushed-rock embankment (USACCE), having crushed-rock revetment on the two side-slopes and crushed-rock interlayer on the base (Figure 1), is one of main structure of the ACCE along the QTR in permafrost regions. The cooling effects of it not only include Raleigh–Bernard convection mentioned above, but also include wind-forced convection in the crushed-rock interlayer (Wu et al., 2007).

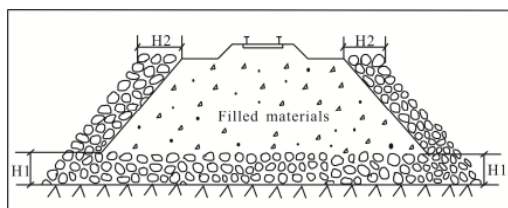


Figure 1. Sketch map of U-shaped air-convection crushed-rock embankment

However, although permafrost is a geologic manifestation of climate (Brown, 1973), its distribution and thermal condition can be influenced by site-specific factors, such as solar radiation, vegetation, snow, soil moisture and so on (Williams and Smith, 1989). Roadway construction in permafrost regions will change some of those site-specific factors, thereby breaking the ground-surface energy balance and then disturbing the thermal conditions of ground surface and underlying permafrost. For the QTR construction, the vegetation removal and construction activity severely changed the thermal regime underneath, and meanwhile more attention should be paid to the thermal effects related to the two embankment side-slopes (Cheng et al., 2003). The different aspects of the two side-slopes could impact the thermal conditions within the embankment and underlying permafrost considerably. First, the different aspects could lead to different magnitudes of solar radiation absorbed by the two side-slopes. It should be noted that the combination of low latitude, high elevation, thinner atmosphere and higher atmosphere transparency makes the Qinghai-Tibet Plateau an area with the strongest solar radiation on the earth (Chen et al., 2006;), implying that significant differences in solar radiation on the two side-slopes can exist. Second, the different aspects can also impact the wind-forced convection within the crushed-rock layer of the USACCE over winter time. Since 75% of strong winds occur in winter on QTP with dominant direction of northwest (Wu et al., 2003;), these two side-slopes would be windward slope and leeward slope respectively over winter time if the embankment orientation is or near northeast to southwest. The strong wind-forced convection on the windward slope and relatively weak wind-forced convection on the leeward slope can lead to considerable thermal differences beneath these two side slopes (Lai et al., 2006; Wu et al., 2007). So substantial thermal differences between two slopes of USACCE can exist, and then result in an asymmetric thermal regime within and beneath the embankment. In permafrost regions, this asymmetric temperature regime within and beneath the embankment will definitely result in a

different deformation in the embankment, leading to some embankment disasters and thus undermining the stability of the embankment (Ma et al., 2008b, 2009). So, more study should be done on those thermal differences for future strengthening measure to diminish those thermal differences.

Based on in situ ground temperature data from long-term monitoring system of the QTR, this paper investigated the thermal differences between right and left portions of the embankment with different orientations and located in different permafrost regions. Three representative monitoring sites were chosen to analysis temperatures, n factors, freezing and thawing indices of near-surface grounds on the right and left embankment shoulders and the natural grounds nearby. Then the thermal regime within and beneath the embankment was examined by comparisons of ground temperature profiles of the embankment shoulders and the natural grounds. By the analysis and the comparisons, the relationship between the thermal differences and solar radiation and wind-convection of the USACCE were discussed qualitatively.

2 MONITORING SITES AND METHOD

In order to study the relationships between the thermal differences and solar radiation and wind-forced convection of the USACCE, the embankment orientation and location of the monitoring sites were taken into account. First, the orientations of the embankment at three chosen monitoring sites are near north to south, east to west and northeast to southwest respectively. For an embankment with orientation of near east to west, along QTR from Golmud to Lhasa, the right slope is sunny and windward slope while left slope is shady and leeward. Second, with respect to wind-forced convection of the USACE, previous studies showed that the cooling effect of the ACCE was related to the mean annual ground temperature (MAGT) of the permafrost at the embankment locations: in regions with lower MAGT ($TCP < -1.0\text{ }^{\circ}\text{C}$), the cooling effect of ACCE was stronger and effective, whereas in regions with higher MAGT ($TCP > -1.0\text{ }^{\circ}\text{C}$), the ACCE provided a relatively weak cooling effect (Ma et al., 2008a; Mu et al., 2010). So, the three chosen monitoring sites are respectively positioned in permafrost regions with different MAGTs. The crushed-rock revetment and crushed-rock interlayer of the USACCE are 0.8 m (H2) and 1.2 m (H1) in thickness, respectively. The diameter of crushed-rock is 0.3-0.4 m. The detailed information of three monitoring sites is described in Table 1.

Typically, four boreholes were drilled at every monitoring site to monitor long-term ground temperatures not only within and beneath embankment but also in natural ground. These boreholes, as shown in Figure 2, include natural borehole, left shoulder borehole, right shoulder borehole, and central borehole. The natural borehole is 18 m in depth and 20 m laterally far from the embankment toe. The left shoulder borehole, the right shoulder borehole and the central borehole are 20 m deep from the embankment surface. Ground temperatures at each borehole were measured with

thermistors attached to data loggers. In every borehole a thermistor cable, with thermistors at 0.5 m intervals, was installed in a galvanized iron pipe which was plugged into the borehole after drilling. The thermistors, with a precision of ± 0.05 °C, were made by State Key Laboratory of Frozen Soil Engineering, China; and ground temperature data were automatically collected by data logger (DT500) on a daily basis.

Table 1. Detailed information of three monitoring sites.

MS ¹	Longitude Latitude	MAGT (°C)	NPT ² (m)	HE ³ (m)	ES ⁴
P15	E93°01.694' N35°04.066'	-1.28	2.3	3.0	204.8°
P25	E92°20.375' N34°00.675'	-0.74	2.4	3.4	174.5°
P30	E92°14.064' N33°46.399'	-0.46	2.7	5.7	243.8°

¹. MS: monitoring site

². NPT: natural permafrost table

³. HE: height of embankment

⁴. ES: embankment strike

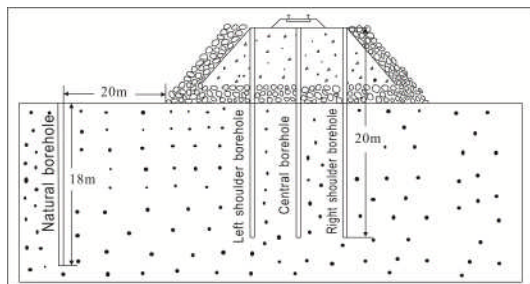


Figure 2. Distribution of the borehole at typical monitoring site

3 RESULTS AND DISCUSSION

3.1 Thermal conditions of ground surface on the embankment and the natural ground

Site-specific factors including micro-topography, vegetation, snow cover, soil moisture and substrate properties will intensively impact ground surface temperature (GST). Snow cover effect, although a principal source of the temperature difference between the air and ground in permafrost regions, can be neglect because of dry and windy winter on the Qinghai-Tibet Plateau (Cheng et al., 2008). Compared to natural ground, the embankment surface has no vegetation cover and two side-slopes are covered by crushed-rock revetment. Meanwhile, the filled materials in the embankment are different from natural grounds; their moisture contents are obvious lower than that of the natural grounds. Therefore, the annual range of the GST on the embankment is always larger than that in the natural ground; in summer, the GST on the embankment is higher than that on the natural ground since direct solar radiation; in winter, the opposite is true as a consequence

of no thermal insulation layer as vegetation cover on the embankment and of cooling effect provided by the crushed-rock revetment. Differences in the annual range of the GSTs can be clearly manifested by the annual amplitude of ground surface on the embankment shoulders and the natural ground. In Table 2, the annual amplitudes of the ground surface on the embankment shoulders were obviously larger than that on the natural ground at monitoring sites P15, 25 and 30 from 2005 to 2008.

Monitoring site P15 is located at upland between Kekexili Mountain and Hongliang River and the MAGT there is -1.28 °C. The annual amplitude of the ground surface on the right shoulder was 3 °C and 5 °C larger than that on the left shoulder and the natural ground, respectively (Table 2). The GSTs on the embankment shoulders and the natural ground from October 2005 to December 2008 are plotted contrastively in Figure 3. It can be found that GSTs on the embankment shoulders were higher than that on natural ground over summer time while the opposite was true over winter time. Meanwhile the differences in GSTs on the two embankment shoulders were slight over summer time but obvious over winter time. These differences were related to the embankment orientation. As described in Table 1, the embankment orientation at this site was 204.8°. Thus, the differences in the magnitudes of solar radiation absorbed by the left and right side-slopes were not obvious over summer time, leading to the slight differences. But over winter time, the right side-slope was a windward slope and the left slope was a leeward slope, consequently the cooling effect was stronger on right side-slope than on left side-slope, leading to the obvious differences. In Table 3, the averages of GSTs on the left shoulder and the natural ground were almost identical while that on the right shoulder was about 0.8 °C lower than the two former temperatures.

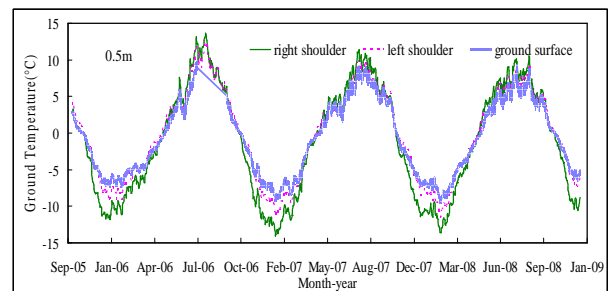


Figure 3. GSTs at monitoring site P15 from October 2005 to December 2008.

Monitoring site P25 is located on south slope of Kexinling Mountain with a MAGT of -0.74 °C. At this site, the annual amplitude of the ground surface on the right shoulder was about 1 °C and 2 °C larger than those on the left shoulder and the natural ground, respectively. In contrast to the conditions at monitoring site P15, the differences in GSTs on the right and left embankment shoulders and the natural ground at this site were slight both over summer and winter time (Figure 4). As the

orientation of the embankment here is 174.5° (Table 1), the solar radiations on the two side-slopes are almost same all year long. Meanwhile, the cooling effect of the USACCE at this site was not strong and moreover the orientation of the embankment is almost parallel with the dominant wind direction on the QTP, meaning near same cooling effects on the two side-slopes over winter time. Thus the GSTs on the right and left shoulders had no obvious difference, which also can be found in Table 3 wherein the annual average of the GST on the right shoulder was only 0.3°C higher than that on the left shoulder.

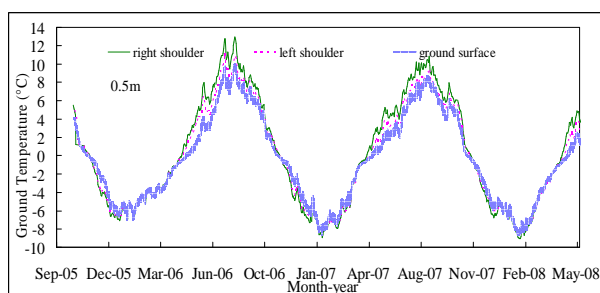


Figure 4. GSTs at monitoring site P25 from October 2005 to May 2008.

Monitoring site P30 is located at billabong on the west bank of Buqu River with the MAGT of -0.48°C . At this site, the annual amplitude of ground surface on the right shoulder was about 1°C and 4.5°C greater than those on the left shoulder and the natural ground. The GST on the right shoulder was obvious lower than that on the left shoulder all year long (Figure 5), which was the corporate results of the solar radiation and cooling effect of the USACCE. As the orientation of the embankment at this site is 243.8° , near east to west, the right slope becomes shady and a windward slope whereas the left slope is sunny and a leeward slope. From Table 3, it can be found that the annual average of the GST on the right shoulder was about 1.8°C lower than that on the left shoulder.

Tables 4 and 5 presented the freezing and thawing indices and n-factors of the near-surface grounds on the embankment shoulders and the natural ground at three monitoring sites from 2005 to 2008.

The freezing and thawing indices of the near surface grounds on the embankment shoulders were all greater than that of the natural ground at the three monitoring sites (Table 4), corresponding with the annual amplitude of the ground surface. For monitoring site P15, the absolute value of the thawing indices and freezing indices on the right shoulder were about $100^\circ\text{C}\cdot\text{days}$ and $350^\circ\text{C}\cdot\text{days}$ larger than these on the left shoulder, respectively. For monitoring site P25, the differences of the freezing and thawing indices on the right and left shoulders and natural ground were slight, excepting the thawing indices on right shoulder being relatively larger than those on the left shoulder and the natural ground. For monitoring site P30, the thawing indices on the left shoulder was about $300^\circ\text{C}\cdot\text{days}$ and $700^\circ\text{C}\cdot\text{days}$ larger than that on the right shoulder and natural ground

respectively, while the absolute value of the freezing indices on the right shoulder was around $300^\circ\text{C}\cdot\text{days}$ larger than those on the left shoulder and the natural ground. The freezing indices and thawing indices conditions above well demonstrate the temperature differences between near-surface grounds on the right and left shoulders and the natural ground over winter and summer times.

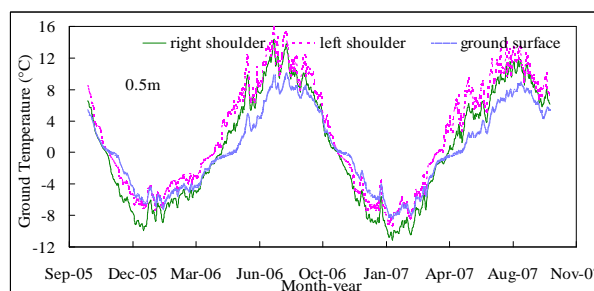


Figure 5. GSTs at monitoring site P30 from October 2005 to October 2007.

The freezing and thawing n-factors of the near-surface grounds on the embankment shoulders were also all larger than those on the natural grounds at the three monitoring sites (Table 5). For the natural grounds, the freezing n-factors ranged from 0.36 at monitoring site P30 to 0.46 at monitoring site P15, which corresponds with the MAGT of the monitoring site. For embankment shoulders, the range of the freezing n-factors was 0.37–0.68, and the differences between the factors on the right shoulder and the left shoulder were 0.17, 0.02, and 0.15 respectively at monitoring site P15, P25, P30, well reflecting the thermal differences between the two shoulders over winter time. The thawing n-factors on natural ground ranged from 0.9 (monitoring site P15) to 1.23 (monitoring site P25), while those on embankment shoulders ranged from 1.05 (monitoring site P15) to 1.82 (monitoring site P30). The differences between the thawing n-factors on the right shoulder and the left shoulder were 0.12, 0.02, and -0.41 respectively at monitoring site P15, P25, P30, also indicates the thermal difference between the two shoulders over summer time. By analysis of the thermal conditions of near-surface grounds on the embankment shoulders and natural ground at three monitoring sites above, we found that the thermal differences between near-surface grounds on the right and left shoulders were dominated by solar radiation in summer time and by both solar radiation and cooling effect of the USACE in winter time. And these thermal differences were closely related to the embankment orientation and MAGT of the region the embankment located in. At three monitoring sites, the thermal differences were slightly for monitoring site P25, but obvious for monitoring site P15 with the cooling effect of the USACE as a major determinant, and more obvious for monitoring site P30 under double effects of the solar radiation and the cooling effect of the USACE.

Table 2. Annual amplitude of the GST at three monitoring site. (°C)

Time (year. month)	Monitoring site P15			Monitoring site P25			Monitoring site P30		
	Left shoulder	Right shoulder	Natural ground	Left shoulder	Right shoulder	Natural ground	Left shoulder	Right shoulder	Natural ground
2005.11-2006.10	18.01	21.18	15.67	14.77	16.33	13.8	18.3	19.35	14.33
2006.11-2007.10	18.47	22.25	15.9	15.67	16.98	14.52	18.84	19.85	15.25
2007.11-2008.10	17.09	19.91	14.86	15.85	16.17	14.82			

Table 3. Annual average of the GSTs at three monitoring sites form 2005 to 2008. (°C)

Time (year. month)	Monitoring site P15			Monitoring site P25			Monitoring site P30		
	Left shoulder	Right shoulder	Natural ground	Left shoulder	Right shoulder	Natural ground	Left shoulder	Right shoulder	Natural ground
2005.11-2006.10	0.43	-0.41	0.3	0.93	1.35	0.44	2.56	0.79	0.52
2006.11-2007.10	-0.32	-1.12	-0.18	0.41	0.87	0.26	2.1	0.32	0.2
2007.11-2008.10	-0.53	-1.25	-0.58	0.12	0.11	0			

Table 4. Freezing and thawing indices at three monitoring sites form November 2005 to October 2008. (°C·days)

Monitoring sites and position		2005.11~2006.10		2006.11~2007.10		2007.11~2008.10	
		Freezing indices	thawing indices	Freezing indices	Thawing indices	Freezing indices	Thawing indices
P15	left shoulder	-902.59	1072.98	-1056.08	953.22	-1055.27	868.78
	right shoulder	-1251.7	1116.68	-1442.15	1053.39	-1415.79	968.44
	natural ground	-815.56	927.22	-917.1	909.72	-950.22	747.19
P25	left shoulder	-693.76	1043.59	-798.95	965.59	-833.33	864.39
	right shoulder	-707.45	1212.78	-819.56	1156.54	-902.16	879.23
	natural ground	-660.36	827.16	-707.42	819.34	-773.41	779.96
P30	left shoulder	-631.95	1593.62	-776.54	1518		
	right shoulder	-978.42	1295.79	-1077.66	1171.41		
	natural ground	-690.94	893.17	-748.32	814.2		

Table 5. N-factor of the near-surface grounds at three monitoring sites.

	Freezing n-factor			Thawing n-factor		
	Left shoulder	Right shoulder	Natural ground	Left shoulder	Right shoulder	Natural ground
P15 (07.11~08.10)	0.51	0.68	0.46	1.05	1.17	0.9
P25 (07.11~08.10)	0.42	0.46	0.39	1.25	1.27	1.23
P30 (06.11~07.10)	0.37	0.52	0.36	1.82	1.41	0.98

Table 6. Annual ground temperature at two different depth in and beneath embankment. (°C)

Time	P15 (1.8m/3.5m)		P25 (2.2m/3.9m)		P30 (4.5m/6.2m)	
	Left shoulder	Right shoulder	Left shoulder	Right shoulder	Left shoulder	Right shoulder
2005.11~2006.10	-0.47/-0.66	-1.65/-1.48	0.41/0.07	0.43/0.02	0.28/-0.05	-0.76/-0.5
2006.11~2007.10	-0.81/-0.74	-2.06/-1.64	0.13/0.02	0.16/-0.05	0.15/-0.02	-0.92/-0.66
2007.11~2008.10	-0.94/-0.83	-2.09/-1.6	-0.07/-0.08	-0.09/-0.17		

Table 7 Permafrost table conditions under embankment at three monitoring sites by 2008. (m)

Monitoring site	Natural permafrost table	Artificial permafrost table		Uplift of permafrost table	
		Left shoulder	Right shoulder	Left shoulder	Right shoulder
P15	2.3	3.3	3.2	2.0	2.1
P25	2.4	4.0	4.0	1.8	1.8
P30	2.6	6.1	4.5	2.2	3.8

3.2 Thermal conditions within and near the natural ground surface under the embankment

The thermal differences between near-surface grounds on the left and right shoulders, accumulating along the embankment downward, resulted in different thermal regimes within the embankment. Figures 6 to 8 presented the ground temperatures within the embankment and near the natural ground surface at three monitoring sites. The temperatures presented in the figures were respectively at two different depths; the first depth was at the top of the crushed-rock interlayer in the embankment, and the second depth was 0.5 m below the natural ground surface under the embankment. For example, in Figure 6, “left 1.8 m” stood for ground under left shoulder at 1.8 m depth, and this depth was just at the top of crushed-rock interlayer; “left 3.5 m” represented ground under left shoulder at 3.5 m depth, and this depth was 0.5 m immediately below the natural ground surface. In the following, the thermal conditions at these two depths are discussed and analyzed.

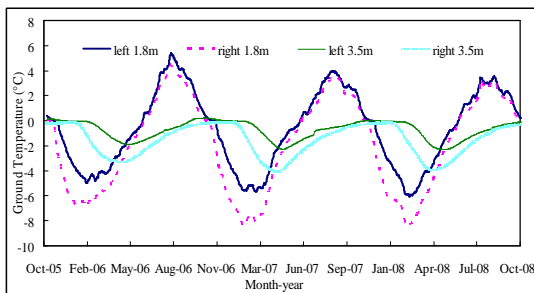


Figure 6 Temperatures of the grounds at depths of 1.8m and 3.5m under embankment shoulders at monitoring site P15.

For monitoring site P15 (Figure 6), at 1.8 m depth, the ground temperatures under the right shoulder was all along lower than that under the left shoulder, and the difference between them was greater in winter while smaller in summer; the average annual temperature of the ground under the right shoulder was about 1.2 °C lower than that under the left shoulder (Table 6). At 3.5 m depth, near the permafrost table under the embankment, the ground temperatures under right and left shoulders were near 0 °C with no obvious difference in warm seasons, but in cold seasons the ground temperature under right shoulder was obviously lower than that under left shoulder; the average annual temperature of the ground under the right shoulder was 0.8 °C lower than that under the left shoulder (Table 6).

For the monitoring site P25 (Figure 7), both at 2.2 m and 3.9 m depths, the differences between ground temperatures under the right and left shoulders were very small and thus the average values of the ground temperatures of them were almost equal with differences less than 0.1 °C.

For monitoring site P30 (Figure 8), also at two depths, the ground temperatures under right and left shoulders

had obvious differences. At depth of 4.5 m, the temperature difference of the grounds under right and left shoulders came from all year long. This was in contrast to the condition at the depth of 6.2 m where the ground temperature difference under the right and left shoulders mainly came from the winter time. The annual average of the ground temperatures at 4.5 m depth under right and left shoulders had a difference about 1 °C while the difference at 6.2 m depth was about 0.5 °C. The freezing and thawing indices of the grounds at these two depths under right shoulder and left shoulder were different considerably.

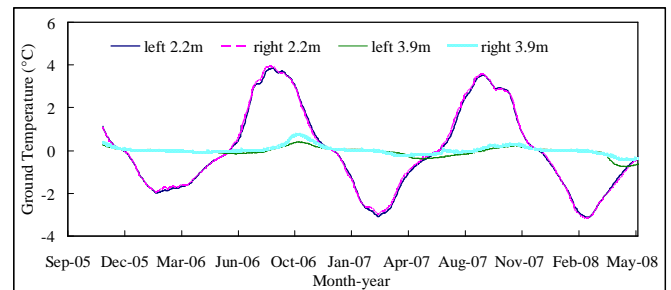


Figure 7. Temperatures of the grounds at depths of 2.2m and 3.9m under embankment shoulders at monitoring site P25.

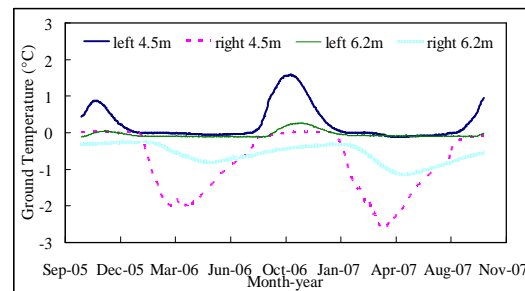


Figure 8. Temperatures of the grounds at depths of 4.5m and 6.2m under embankment shoulders at monitoring site P30.

3.3 Thermal conditions of the permafrost beneath the embankment

As the principal support layer of the load on the embankment, the thermal regime of underlying permafrost is a crucial factor determining the embankment stability and deformation. For the three monitoring sites, two different thermal regimes in underlying permafrost were experienced which were induced by ground surface conditions analyzed above, and are analyzed in detail as following.

First, a symmetric thermal regime of permafrost beneath the embankment existed at monitoring site P25. At the site, after the embankment built, the permafrost table had been uplift by 1.8 m both under the right and the left shoulders by 2008. And the grounds between the

permafrost table and 8 m depth under the two shoulders had a slightly cooling trend, but the grounds deeper warmed slightly but steadily with time (Figure 9). Compared to the natural ground, the permafrost under the right and left shoulders were slightly colder and almost had no temperature differences between each other (Figure 12b). The permafrost temperature at 14 m depth under the right shoulder, the left shoulder and the natural ground were $-0.66\text{ }^{\circ}\text{C}$, $-0.64\text{ }^{\circ}\text{C}$, $-0.63\text{ }^{\circ}\text{C}$, respectively. So, the thermal regimes beneath the embankment shoulders were near symmetric, and this was good for the stability of the embankment.

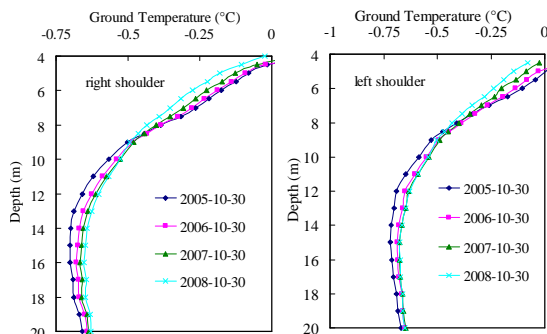


Figure 9. Permafrost temperature profiles beneath the left and right shoulders at monitoring site P25

Second, asymmetric thermal regimes of permafrost beneath the embankments existed at monitoring sites P15 and P30.

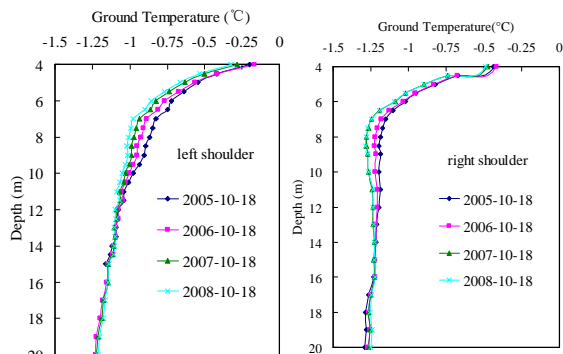


Figure 10. Permafrost temperature profiles beneath the left and right shoulders at monitoring site P15

For monitoring site P15, the permafrost table under right and left shoulders had upgraded about 2.0m and 2.1m respectively from the time embankment built to 2008, and was near the natural ground surface, meaning that almost no active layers exist beneath the embankment. During the period, the ground beneath the permafrost table to 12 m depth under the embankment shoulders had an obvious and steady cooling trend while the deeper grounds were thermal stable almost with no temperature changes (Figure 10). In comparison between temperature profiles beneath the embankment shoulders

and the natural ground (Figure 12a), it can be clearly found that the permafrost beneath the embankment shoulders were colder than that beneath the natural ground, displaying a strong cooling effect of the USACE. But it should be note that the permafrost temperatures under the right shoulder and the left shoulder were considerably different. For example, the permafrost temperatures at 14 m depth under the right shoulder, the left shoulder and the natural ground were $-1.22\text{ }^{\circ}\text{C}$, $-1.1\text{ }^{\circ}\text{C}$ and $-1.0\text{ }^{\circ}\text{C}$, respectively. Combining with the analysis of the near-surface ground thermal differences, we found that although the contribution of the solar radiation to the thermal differences between the grounds under left and right shoulder was relatively small, the strong cooling effect of the USACE still could lead to a considerable asymmetric thermal regime beneath the embankment.

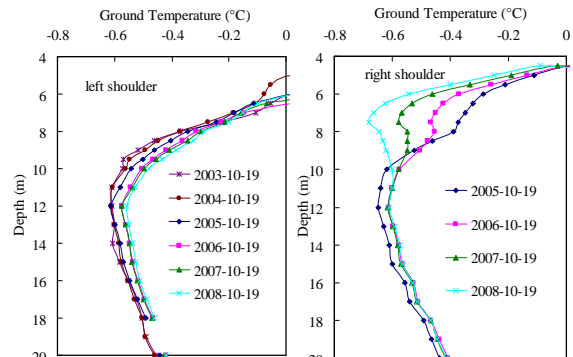


Figure 11. Permafrost temperature profiles beneath the left and right shoulders at monitoring site P30.

For monitoring site P30, since the high embankment, the permafrost table under the embankment shoulders had larger upward movement than that at the two former monitoring sites. The upward movement of the permafrost table under the right shoulder was 3.8 m while that under the left shoulder was 2.2 m (Table 7). The thermal conditions of the permafrost under the right and left shoulders were clearly different; all the permafrost under the left shoulder had a warming trend of about an order of $0.1\text{ }^{\circ}\text{C}$, while the permafrost under the right shoulder from the permafrost table to 10 m depth had an obvious cooling trend. From the comparison of temperature profiles beneath the embankment shoulders and natural ground (Figure. 12c), it can be found that the permafrost temperature beneath the embankment shoulders were still lower than that beneath the natural ground. Also, it can be found that shallow permafrost temperatures between the depths of 4 m and 12 m under the right shoulder were substantial lower than that under left shoulder. So, the thermal regime under embankment, simultaneously influenced by solar radiation and cooling effect of the USACE, was severe asymmetric than that at monitoring site P25 and would definitely lead to great different deformation in the embankment. Furthermore, with respect to the increase of the thawing indices and decrease of the freezing indices of the near-surface ground on the left shoulder (Table 4), the permafrost under the left shoulder would warm in future;

consequently the asymmetric under the embankment would be more severe.

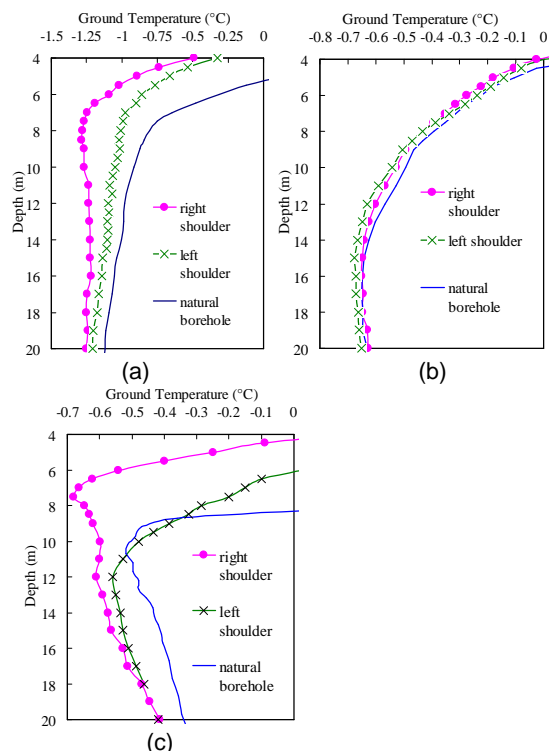


Figure 12. Comparisons of temperature profile of embankment shoulders and the natural boreholes. (a), P15; (b) P25; (c) P30.

4 CONCLUSION

By analyzing the thermal differences between right and left portions of USACE, this paper found that the major determinants for the thermal differences include the solar radiation and wind-forced convection of the USACE. Thus the thermal differences were closely related to the embankment orientation and the dominant wind direction. If the two determinants work together, a severe asymmetrical thermal regime within and beneath the embankment would exist, such as monitoring site P30, and then some remedy measures should be done to diminish this thermal difference to keep embankment stability. But it should be noted that although the contribution of solar radiation to the thermal differences between the right and left shoulders was small, the different intensity of wind-forced convection on the right and left portions of the embankment still could result in a asymmetrical thermal regime within and beneath the embankment, such as monitoring site P15. So, placing crushed-rock revetment with different width on two sideslopes can diminish the thermal differences on them.

ACKNOWLEDGEMENTS

This work was support by the grant of the Western Project Program of the Chinese Academy of Sciences

(Grant No. KZCX2-XB2-10), the Program for Innovative Research Group of Natural Science Foundation of China (Grant No. 40821001), the National Natural Science Foundation of China (No. 40801022), the China Postdoctoral Science Foundation (No. 200902312) and the Foundation of the State Key Laboratory of Frozen Soils Engineering, CAS. (Nos. SKLFSE-ZY-03 and SKLFSE-ZQ-02).

REFERENCES

- Brown, R.J.E., 1973. Influence of climatic and terrain factors on ground temperatures at three locations in the permafrost region of Canada, In 2nd International Conference on permafrost, proceedings, North American Contribution, pp. 27-34.
- Chen, J., Hu, Z.Y., Dou, S. and Qian, Z.Y., 2006. Yin-Yang Slope problem along Qinghai-Tibetan Lines and its radiation mechanism. *Cold Regions Science and Technology*, 44(2006): 217-224.
- Cheng, G.D., 2004. Influences of local factors on permafrost occurrence and their implications for Qinghai-Tibet Railway design. *Science in China Series D*, 47(5): 704-709.
- Cheng, G.D., Jiang, H., Wang, K.L. and Wu, Q.B., 2003. Thawing Index and Freezing Index on the Embankment Surface in Permafrost Regions. *Journal of Glaciology and Geocryology*, 25(6): 603-607.
- Cheng, G.D., Lai, Y.M., Sun, Z.Z. and Jiang, F., 2007. The 'Thermal Semi-conductor' Effect of Crushed Rocks. *Permafrost and Periglacial Processes*, 18(2): 151-160.
- Cheng, G.D., Sun, Z.Z. and Niu, F.J., 2008. Application of the roadbed cooling approach in Qinghai-Tibet railway engineering. *Cold Regions Science and Technology*, 53(3): 241-258.
- Cheng, G.D. and Tong, B.L., 1978. Experimental research on an embankment in an area with massive ground ice at the lower limit of alpine permafrost, Proceedings of the 3rd International Conference on Permafrost. National Research Council of Canada, Ottawa, pp. 199-222.
- Goering, D.J. and Kumar, P., 1996. Winter-time convection in open-graded embankments. *Cold Regions Science and Technology*, 24(1): 57-74.
- Goering, D.J., 2003. Passively cooled railway embankments for use in permafrost areas. *Journal Cold Regions Engineering*, 17(3): 119- 133.
- Lai, Y.M., Zhang, M.Y., Liu, Z.Q. and Yu W.B., 2006. Numerical analysis for cooling effect of open boundary ripped-rock embankment on Qinghai-Tibetan railway. *Science in China: Series D Earth Sciences* 49(7) : 764-772.
- Ma, W., Cheng, G.D. and Wu, Q.B., 2009. Construction on permafrost foundations: Lessons learned from the Qinghai-Tibet railroad. *Cold Regions Science and Technology*, 59(1): 3-11.
- Ma, W., Feng, G.L., Wu, Q.B. and Wu, J.J., 2008a. Analyses of temperature fields under the embankment with crushed-rock structures along the Qinghai-Tibet Railway. *Cold Regions Science and Technology*, 53(3): 259-270.

- Ma, W., Qi, J.L. and Wu, Q.B., 2008b. Analysis of the deformation of embankments on the Qinghai-Tibet Railway. *Journal of Geotechnical and Geoenvironmental Engineering*, 134(11): 1645-1654.
- Ma, W., Shi, C.H., Wu, Q.B., Zhang, L.X. and Wu, Z.J., 2006. Monitoring study on technology of the cooling roadbed in permafrost region of Qinghai-Tibet plateau. *Cold Regions Science and Technology*, 44: 1-11.
- Mu Yanhu, Ma Wei, Liu Yongzhi, Sun Zhizhong., 2010. Monitoring investigation on thermal stability of air-convection crushed-rock embankment. *Cold Regions Science and Technology*, 62(2-3):160-172.
- Wu, Q.B., Cheng, G.D. and Ma, W., 2003. The impact of permafrost change on the Qinghai-Tibet Railway. *Science in China, Series D: Earth Sciences*, 33(Special Issue): 114-122.
- Wu, Q.B., Cheng, H.B., Jiang, G.L., Ma, W. and Liu, Y.Z., 2007. Cooling mechanism of embankment with block stone interlayer in Qinghai-Tibet railway. *Science in China Series E: Technological Sciences*, 50(3): 319-328.
- Wu, Q.B., Lu, Z.J., Zhang, T.J., Ma, W. and Liu, Y.Z., 2008. Analysis of cooling effect of crushed rock-based embankment of the Qinghai-Xizang Railway. *Cold Regions Science and Technology*, 53(3): 271-282.
- Williams PJ, Smith MW. 1989. *The Frozen Earth. Fundamentals of Geocryology*. Cambridge University Press: Cambridge; 306.